sustainability

MDPI

Article

Investigating the Effect of Processing Parameters on the Products of Hydrothermal Carbonization of Corn Stover

Ibrahim Shaba Mohammed [1], Risu Na [1], Keisuke Kushima [1] and Naoto Shimizu [2,*]

[1] Graduate school of Agriculture, Hokkaido University, 9-9 Kita, Kita-ku, Sapporo, Hokkaido 060-8589, Japan; shabamohammed4real@yahoo.co.uk (I.S.M.); narisu0299@yahoo.co.jp (R.N.); kushimakeisuke@eis.hokudai.ac.jp (K.K.)

[2] Research Faculty of Agriculture, Hokkaido University, 9-9 Kita, Kita-ku, Sapporo, Hokkaido 060-8589, Japan

* Correspondence: shimizu@bpe.agr.hokudai.ac.jp; Tel.: +81-(0)-11-706-3848

Received: 12 May 2020; Accepted: 19 June 2020; Published: 23 June 2020

Abstract: Corn stover is an abundant and underused source of lignocellulose waste biomass that can be transformed into a high-quality energy resource using hydrothermal carbonization (HTC). This investigation has focused on the effect of processing parameters on the products of HTC—namely solid fuel or hydrochar and liquid and gas fractions. HTC was conducted in a temperature-controlled small batch reactor with corn stover and deionized water under oxygen-free conditions obtained by pressurizing the reactor headspace with nitrogen gas. The properties of the hydrochar and liquid and gas fractions were evaluated as a function of the process temperature (250–350 °C), residence time (30–60 min) and biomass/water ratio (0.09–0.14). Central composite design modules in a response surface methodology were used to optimize processing parameters. The maximum mass yield, energy yield and high heating value (HHV) of the hydrochar produced were 29.91% dry weight (dw), 42.38% dw and 26.03 MJ/kg, respectively. Concentrations of acetic acid and hydrogen gas were 6.93 g/L and 0.25 *v/v*%, respectively. Experimental results after process optimization were in satisfactory agreement with the predicted HHV. The optimal HTC process parameters were determined to be 305 °C with a 60 min residence time and a biomass/water ratio of 0.114, yielding hydrochar with a HHV of 25.42 MJ/kg. The results confirm the feasibility of an alternative corn stover management system.

Keywords: corn stover; hydrochar; hydrothermal liquid; gas fraction; bioenergy management system

1. Introduction

Biomass is the waste and residual biological material of plants and animals [1]. The application of lignocellulose biomass as a sustainable resource has gained traction to achieve a reduction in greenhouse gas emissions [2]. Near-zero greenhouse gas emissions can be accomplished by balancing plant biomass production and use in the future [3]. Bioenergy is a potential renewable energy and low-emissions resource, and is sustainable if its social impact, economics and environment are well managed [4]. Lignocellulose biomass is recognized as an essential source of renewable energy because of its universal availability, low cost, flexible application (energy or heat production) and carbon neutrality [5]. However, the capital costs and labor-intensive pretreatment and processing requirements associated with utilizing lignocellulose biomass must be addressed before any technique can become widely adopted [6].

Numerous literatures have made conclusions regarding the upgrade of biomass combustion properties such as their hydrophobic nature, combustion efficiencies, heating values, moisture content and energy density. Torrefaction significantly improves the combustion properties of lignocellulose

biomass with respect to the aforementioned properties, but a degree of uncertainty exists in torrefaction, particularly involving a decrease in alkali contents from agricultural residuals [7] and a gradual breakdown of mill performances in the grinding of torrefied biomass. These challenges result in corrosion, agglomerations and a reduction in combustion efficiencies due to high percentages of unburned carbon in fly ash. Valorization via hydrothermal carbonization (HTC) is particularly suitable for biomass residues with high proportions of inorganic elements (a high mass fraction of ash content). The benefit of hydrothermal biomass conversion techniques is that they do not demand drying of biomass, which reduces energy requirements and process expenditure. The hydrothermal conversion process itself is cost-effective when compared to other conventional thermal drying techniques [8]. HTC has received significant attention for converting high moisture biomass to coal-like materials (solid fuel) with a reduced inorganic content. For example, HTC has been applied in the production of solid fuels with high energy contents using wine industry waste [9], wheat straw [10] tobacco stalks [11], olive mill industry residual biomasses [12], citrus wastes [13] and pulp mill waste [14].

Corn stover is an important source of lignocellulosic biomass in Nigeria, with total production of approximately 200 million tons per year. Because of its carbonaceous nature, corn stover has excellent potential to serve as a raw material to produce coal-like materials [15]. However, the use of corn stover as a solid fuel feedstock is limited by its low energy density, structural heterogeneity, low heating values and high moisture content. With only scant amounts used to feed livestock and in the pulp/paper industries, a huge amount of Nigeria's corn stover is being discarded or combusted, which causes pollution of both the air and the landscape.

HTC is a process of lignocellulose biomass transformation in subcritical or supercritical water under high pressure and temperature in the absence of oxygen, also known as wet pyrolysis. It can be divided into three main stages, namely, gasification, carbonization and liquefaction, which vary based on the processing temperature and residence time. In HTC, a sequence of reactions occurs during lignocellulosic biomass disintegration, including dehydration, hydrolysis, condensation, decarboxylation, aromatization and polymerization [16]. Solid, liquid and gas products are derived from this sequence of reactions. The solid is the main product; it has higher carbon content and increased hydrophobicity relative to the feedstock. The applications of HTC solids include energy storage [17], carbon-based catalysis [18], soil amendment [19], adsorbent [20] and fuel source [21]. The liquid comprises valuable organic chemicals such as acetic acid, glycolic acid, lactic acid, levulinic acid, formic acid, furfural, succinic acid, hydroxymethyl-furfural, furfuryl alcohol and propionic acid. The gas fraction mainly comprises hydrogen, carbon dioxide, methane and carbon monoxide.

Table 1 summarizes previous works of HTC process parameters using a classical experimental design (CED) and responses surface methodology (RSM), as well as solid fuel obtained at supercritical water (SCW) conditions. However, there are limited studies on the production of solid fuel at SCW conditions. Table 1 shows that previous studies utilized CEDs that change one variable at a time and does not reveal the effects of interaction and pure squares between process variables due to a large number of experimental trials, making this approach time consuming. Thus, based on a previous report of compound models, the optimization of solid fuel yield obtained by reducing the number of experimental trials has received insignificant attention in this area of research [22]. In this research, a novel approach to HTC process has been employed to produce a solid fuel with high yields; this fuel is usually examined by optimizing the HTC process parameters mentioned in Table 1. In addition, effects of individual variables, pure squares and their interactions have been estimated by using RSM.

Table 1. Literature review on hydrothermal carbonization (HTC) parameters by using classical experimental design (CED) and responses surface methodology (RSM), solid fuel produced at supercritical water (SCW) conditions made from corn stover.

Previous Work	HTC Parameters Using CED	HTC Parameters by RSM	Solid fuel Produced under SCW Conditions from Corn Stover
Zhu et al. [23]	Temperature (190–320 °C) and hydrothermal treatment severity (4.17–8.28 min)	NA	NA
Machado et al. [24]	Temperature (175–250 °C)	NA	NA
Mosier et al. [25]	Temperature (170–200 °C) and residence time (5–20 min)	NA	NA
Fuertes et al. [26]	Temperature (250 °C)	NA	NA
Xiao et al. [27]	Temperature (250 °C),	NA	NA
Volpe et al. [28]	Temperature (180–250 °C), residence time (0.5–3 h) and biomass/water ratio (0.07–0.30).	NA	NA
Kang et al [29]	NA	Temperature (122.7–257.3 °C), residence time (4.8–55.2 min) and biomass (0.98–6.02 g/50 mL H_2O)	NA
This Study	NA	Temperature (215.91–384.09 °C), residence time (19.8–77 min) and Biomass/water ratio (0.073–0.157)	Solid fuel was produced at SCW conditions

NA: Not Applicable.

RSM is a flexible mathematical method employed in optimization, modeling and experimental design. It is an empirical modeling method that relates one or more responses to independent parameters. It gives statistical indications on individual model terms and interactions [22]. To develop a complete biosystem for the solid fuel, liquid and gas fractions from corn stover must also serve as a pathway to sustainable bioenergy generation. Information regarding the optimization of HTC process parameters by using RSM is limited to the best of our knowledge. Therefore, the aims of this investigation are (1) to optimize conditions and determine the effect of process parameters (the biomass/water ratio, residence time and temperature) on the properties of the hydrochar, (2) to gain insight into the underlying mechanism during HTC, as well as the thermal and structural properties of the hydrochar, and (3) to determine the yield and composition of the liquid and gas fractions, and to assess the feasibility of utilizing them in anaerobic digestion in future work.

2. Materials and Methods

The corn stover (New Dent, 105 days) used in this study was harvested from Hokkaido University Farm. The moisture contents as received were 80 wt%. The collected corn stover was pulverized into a 10 mm square and dried in a ventilated oven at 105 °C for 24 h. This pretreatment was conducted to avoid degradation and begin with a dry reference point. Samples were further milled and sieved to particle sizes of 500 and 800 μm.

2.1. Hydrothermal Carbonization of Corn Stover

HTC was conducted in a temperature-controlled batch reactor (Model: 122841, SUS 316 Tsukuba, Japan) at volumes between 160 and 190 mL. For each experiment, the reactor was charged with 1.09 to 2.36 ± 0.002 g of dried sample (corn stover) and 12.64 to 13.91 ± 0.03 g of deionized water to obtain the desired biomass/water ratio. The experimental layout is detailed in Table 2. Deionized water and corn stover were placed in the batch reactor. Oxygen-free conditions were obtained by pressurizing nitrogen gas to an initial pressure of 4 MPa in the reactor headspace; this also kept the water boiling during the hydrothermal process [30]. Gases were obtained by gas trap bag after the reactor was cooled down. Liquid and solid phases of the reaction solution were separated by vacuum filtration. The liquid

fraction, which is rich in acetic acid, will be used for biogas production in anaerobic fermentation in future work.

Table 2. Variables that were in the central composite design for the hydrothermal hydrochar process.

Factors	Unit	Code Factor Level				
		(-α)	(-1)	(0)	(+1)	(+α)
Temperature	°C	215.91	250	300	350	384.09
Residential Time	h	0.33	0.5	0.75	1	1.17
Biomass/water Ratio	%	0.073	0.09	0.115	0.14	0.157

2.2. Characterization of Raw Corn Stover and Products of HTC

The proximate analysis of raw corn stover and solid fuel was conducted using the ASTM 1762–84 and 3173–87 method. CHN analysis (CE440, Exeter Analytical, Inc, Coventry, UK) was performed to determine the carbon, nitrogen, oxygen and hydrogen content. The high heating value (HHV) of the solid fuels were determined using a digital calorimeter (Model DCS-196, Shinjuku Tokyo, Japan). The thermogravimetric analysis (TGA) of corn stover and the hydrochar were conducted on a Thermo plus EVO II TG 8120 instrument (Rigaku, Tokyo, Japan). A sample (10–15 mg) was heated from ambient temperature to 600 °C at a constant ramp rate of 10 °C min^{-1} under a nitrogen flow rate of 50 mL min^{-1}. The difference in weight after devolatilization and controlled heating was estimated as the weight loss. Surface morphological characteristics of the samples were investigated using a scanning electron microscope (SEM) JSM-6301F system (JEOL, Tokyo, Japan). Samples were place on aluminum stub coated with gold palladium alloys and equal sided carbon tape employing an ion sputtering device (e101 Ion Sputter, Hitachi, Ltd, Tokyo, Japan) before SEM investigation. Investigation was done under high vacuum conditions, $<1.0 \times 10^{-3}$ Pa, at a voltage of 10 kV [31]. The liquid fractions were analyzed using the high-performance liquid chromatography-refraction index (HPLC-RI) 1200 Infinity series with Shodex KS-802 column (Showa Denko, K.K, Tokyo, Japan). Ultrapure water was employed as the mobile phase. The column temperature and flow rate were set to 60 °C and 0.6 mL/min. A solution of 0.3% pullulan standard was used to perform for an alignment peak. The injected volume was 100 µL [31]. Gas chromatography (GC-4000, GL Science, Tokyo, Japan) was used to analyze the gas fraction. CH_4, CO and CO_2 were detected using a GC-FID-TCD interphase (GC with a flame ionization detector and thermal conductivity detector) with hydrogen as the carrier gas. H_2 was detected by GC-TCD [32]. Each of these analyses was replicated three (3) times to minimize errors. The HHV was calculated using the modified Dulong's formula shown below as Equation (1), according to previously published work by Theegala and Midgett [33]. Nitrogen, carbon, hydrogen and oxygen were determined using elemental analysis (although the percentage content of nitrogen is not used in this formula). The mass and energy yield of the hydrochar was obtained from Equations (2) and (3).

$$HHV\left[\frac{MJ}{kg}\right] = \frac{33.5\ X\ wt.\ \%C}{100} + \frac{142.3\ X\ wt.\%H}{100} - \frac{15.4\ X\ wt.\ \%\ O}{100} \quad (1)$$

$$Mass\ Yield = \frac{Mass\ of\ Produced\ Hydrochar}{Mass\ of\ Raw\ Corn\ Stover}\ X100 \quad (2)$$

$$Energy\ Yield = Mass\ Yield\ X\frac{HHV\ of\ Produced\ Hydrochar}{HHV\ of\ Raw\ Corn\ Stover}\ X\ 100 \quad (3)$$

2.3. Experimental Design, Response Surface Methodology Development and Hydrothermal Process Optimization

In this work, process variables (temperature, residence time and biomass/water ratios) that influence the yield of hydrochar were examined using a response surface methodology (RSM). To avoid laying-off (unnecessary repetition of experiments), a central composite design (CCD) was employed to gives 20 experimental trials to study the influence of 3 chosen variables on the solid fuel yield (Table 5).

The range of parameters that were examined are shown in Table 2. Process temperature was assessed in a range from 250 to 350 °C, the biomass/water ratio varied from 0.09 to 0.14 and the residence time varied from 0.5 to 1 h. Three input parameters were investigated at low (−1), medium (0) and high (+1) levels, and axial points were added (axial distances; ± α = 1.68) for design orthogonality. Six center points were utilized to appraise the lack of fits and pure errors of the proposed model. Each of these processes was repeated three times. Multiple regression was employed to fits the coefficients of quadratic model of the response. Quality of the fitted quadratic model was evaluated by using the significances test and analysis of variances (ANOVA). The fitted model is shown in Equation (4).

$$Y = \eta_0 + \eta_1 x_1 + \eta_2 x_2 + \eta_3 x_3 + \eta_4 x_1 x_2 + \eta_5 x_1 x_3 + \eta_6 x_2 x_3 + \eta_7 x_1^2 + \eta_8 x_2^2 + \eta_9 x_3^2 \quad (4)$$

Here, Y is the dependent variable (HHV in MJ/kg), η_0 is the intercept value, η_1, η_2 *and* η_3 are the first order coefficients, η_4, η_5 *and* η_6 are the interaction coefficients, η_7, η_8 *and* η_9 represent the quadratic coefficients and x_1, x_2 *and* x_3 represent the independent parameters.

Local optimization of RSM was utilized to determine the optimum sets of 3 process input variables to maximize HHV. The HHV was set at maximum while the inputs variable was set in the range examined in this study. A desirability function in the RSM module was utilized to search for optimal values which gave the maximum HHV. Predicted optimal value was validated by performing experiments in triplicate using the same conditions as those predicted by RSM. Mean experimental values were compared with the predicted values to assess the precision of prediction [22].

3. Results and Discussion

3.1. Characterization of Solid Fuel, Liquid and Gas Fraction from Corn Stover

3.1.1. Solid Fuel

The composition and energy properties of the raw corn stover and its hydrochar are presented as a function of the processing temperature, residence time and biomass/water ratio in Table 3. For the purpose of comparison, other feedstocks (corn stalk and *Opuntia ficus-indica* cladodes (OC)) are also included in Table 3. The ash content of the hydrochars increased relative to raw corn stover. This observation is contrary to published works on HTC of corn stalk [29] and Miscanthus [34] but in agreement with the study of *Opuntia ficus-indica* cladodes [28]. The ash content of the corn stover hydrochar increases from 18 wt.% of 250 °C, 45 min, to 18.95 wt.% of 300 °C, 77 min, to 25.87 wt.% of 350 °C, 60 min at constant biomass/water ratios of 0.115.The increase in ash content may be caused by reprecipitation of some inorganic material on the solid fuel after a long residence time at high temperatures, as suggested by Kamonwat et al. [35].

The volatile matter (VM) of the raw corn stover obtained was 71.34%, comparable to corn stalk [29] and higher than OC [28]. The VM of the raw corn stover was higher than all the hydrochars produced. The VM in the hydrochar decreased significantly with the increasing processing temperature (250 to 350 °C) at a constant residence time of 60 min and biomass/water ratios of 0.14. This decrease in VM may be attributable to the decomposition of celluloses and hemicelluloses during hydrothermal treatment.

The highest percentage of fixed carbon obtained in the corn stover hydrochar was 31.30% at the processing temperature of 350 °C, residence time of 60 min and biomass/water ratio of 0.14, substantially more than in the hydrochars reported by Cai et al. [11] and Hoekman et al. [36]. High fixed carbon and low volatile matter are more highly desirable characteristics for solid biofuels than raw biomass, which often ignites easily at low temperatures (~250 °C), resulting in rapid maximum weight loss [36]. The increase in temperature (215.9, 300 and 384.09) and residence time (45 and 77 min) at a constant biomass/water ratio of 0.115 enhances the carbon content and decreases the percentages of oxygen and hydrogen. This is a result of decarboxylation and dehydration reactions that take place during HTC, which lead to a decrease in the ratios of O/C and H/C. The ultimate analysis shows that the content of carbon increases gradually with the extension of processing temperature (250 and 350 °C) at

a constant residence time and biomass/water ratio of 60 min and 0.14, respectively. This changed of carbon content trend in hydrochar is consistent with a report developed by Zhu et al. [23].

Table 3. Comparison of average values of proximate analysis, ultimate analysis and energy properties of raw corn stover hydrochar with other types of biomass hydrochars.

Properties	Raw Corn Stover [This Study]	Hydrochars						
		215.9 °C, 0.115, 45 min	250 °C, 0.14, 60 min	300 °C, 0.115, 77 min	350 °C, 0.14 60 min	384.09 °C, 0.115, 45 min	CS [29]	OC [28]
Proximate Analysis (SD ≤ 1.25)								
Volatile Matter (%)	71.34	57.28	60.72	54.47	42.83	40	74.32	56.88
Fixed Carbon (%)	17.67	24.72	19.52	26.58	31.30	30.89	18	28.17
Ash Content (%)	11.05	18	19.75	18.95	25.87	29.11	3.54	14.95
Ultimate Analysis (SD ≤ 1.09)								
Carbon (%)	40.83	52.39	56.67	62.07	57.60	54.18	53.44	50.48
Hydrogen (%)	5.21	4.8	4.76	4.93	4.33	3.7	5.67	4.83
Oxygen (%)	41.38	22.86	16.62	11.52	9.95	10.85	39.64	28.94
Nitrogen (%)	1.54	1.95	2.2	2.53	2.25	2.16	1.12	0.81
O/C	1.01	0.44	0.29	0.19	0.17	0.2	0.74	0.57
H/C	1.28	0.92	0.84	0.79	0.75	0.68	0.106	0.095
Energy Properties (SD ≤ 1.67)								
HHV (MJ/kg)	16.16	22.30	24.20	27.47	25.37	23.75	22.82	22.39
HHV (MJ/kg) [a]	14.72	20.86	23.20	26.03	23.93	21.75		
Energy Yield (%)	1	42.38	22.88	40.90	32.97	29.88	55.70	83

HHV (MJ/kg) [a]: Calculation by formula; CS: Corn Stalk. SD: Standard deviation. OC: Opuntia Ficus-Indica Cladodes.

The atomic ratios quantitative index is an essential standard for assessing the aromatic contents and degree of deoxygenation, during HTC of lignocellulose biomass. The H/C and O/C atomic ratio provide clues about the aromatic contents; a lower ratio of H/C indicates that the aromatic contents of the hydrochar is high. The atomic H/C and O/C ratio of corn stover and its hydrochar are shown in Figure 1. Anthracite, coal, lignite and peat are also presented in the same figure for a coalification comparison. The H/C and O/C ratios of the hydrochar decrease as the residence time and temperature increase. It was obvious that the hydrochar produced at 384.91 °C shows a higher degree of coalification compared to the hydrochars produced at 215.9 °C with a similar residence time and biomass/water ratio, which indicated that demethanation, decarboxylation and dehydration reaction occur during the HTC process, though the rate of reaction of decarboxylation was lower than that of the dehydration. This finding similar to one on the HTC of a high moisture content outlined by Zhu et al. [23]. The hydrochar produced at 300 °C after 77 min with a biomass/water ratio of 0.115 has the highest carbon content of 62.07 wt.% basis; this value is comparable to coal material. Thus, these processing conditions were found to be optimal and would be recommended to produce corn stover hydrochar as a substitute solid fuel for power generation.

Differential thermogravimetric analysis (DTG) and thermogravimetric analysis (TGA) were conducted to examine the thermal disintegration behaviors of raw corn stover and its hydrochar. As presented in Figure 2a, three levels of disintegration were recognized. The first level ranged from 100 to 250 °C and showed gradual weight loss, mostly from the removals of moisture and the release of some volatiles. The second level ranged from 250 to 400 °C and mainly involved the disintegration of cellulose and hemicellulose. At temperatures >450 °C, decomposition was attributed to the slower thermal breakdown of lignin [28]. At 600 °C, the final weight loss of solid fuels increased in the following order: 350 °C < 250 °C < 384.09 °C < 215.91 °C < 300 °C < Raw corn stover.

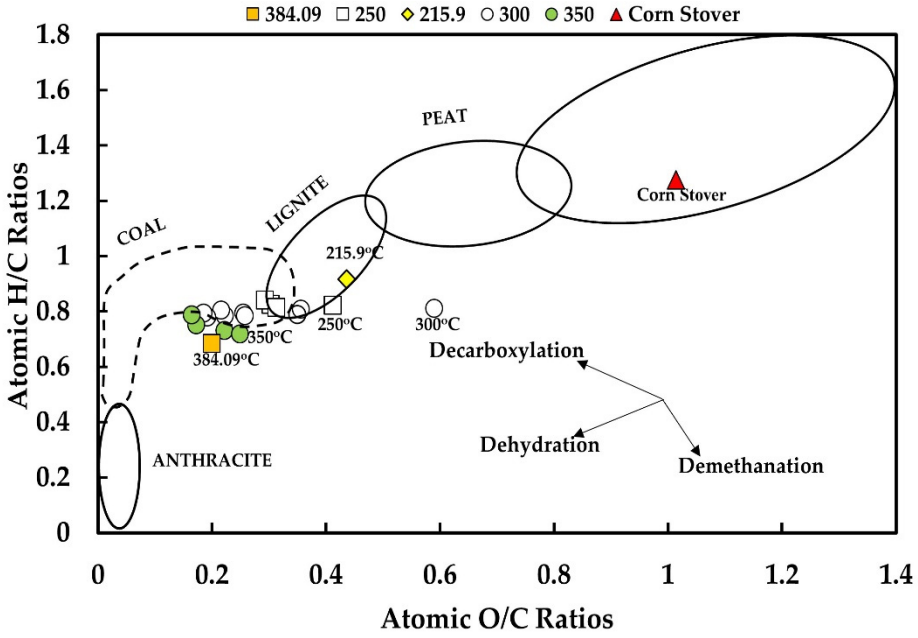

Figure 1. Van Krevelen diagram for raw corn stover and hydrochar.

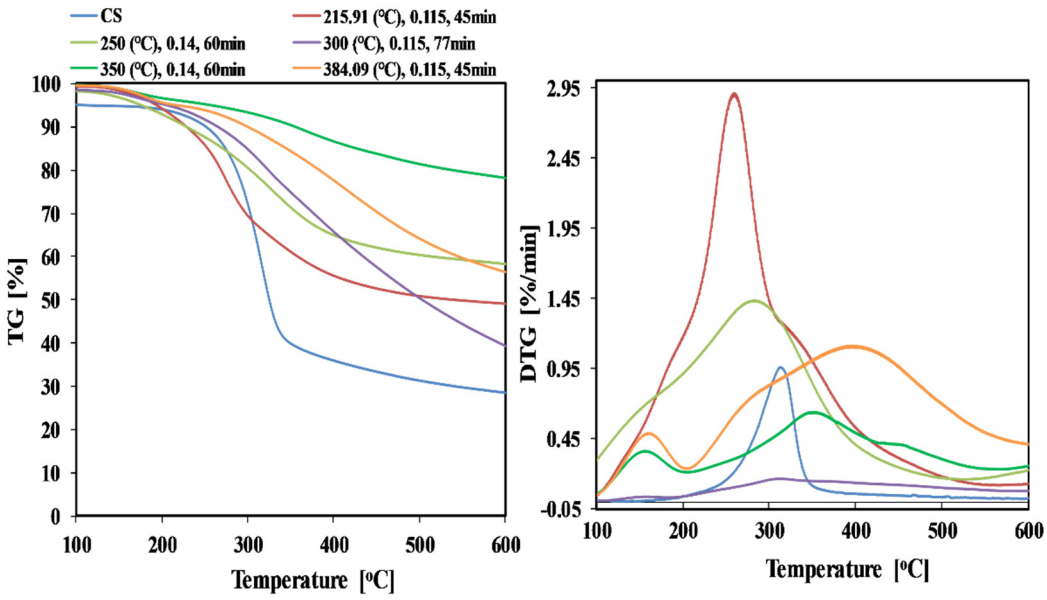

Figure 2. TGA (**a**) and DTG (**b**) Curve of Raw Corn Stover and its Hydrochar.

As shown in Figure 2b, a sharp DTG peak was observed at 320 °C for raw corn stover, likely as a result of the high content of volatile matter. The temperature of the DTG peak increased in line with the increasing processing temperature (250 to 350 °C) and residence time (30 to 60 min) employed in the production of hydrochar. Significant weight loss was not observed for the hydrochar produced at 300 °C, which is likely a result of its high carbon content. As the thermal stability of a solid fuel improves, the air pollution it produces is reduced because of complete combustion [37],

The corn stover and its hydrochars were examined to determine their microstructures (Figure 3) using SEM. The raw corn stover contained a rigid and well organized fibril structure. The hydrochars processed at 215.91 °C and 250 °C depict a rough surface with many discrete droplets where the corn

stover was slowly degraded. As the processing temperature increased to 300 °C and 350 °C, more discrete droplets appear on the surface of the hydrochar, and the droplets gradually increase in size. Finally, granular and molten structures were formed in the hydrochar at a processing temperature of 384.09 °C. The highly organized structure of the raw corn stover is attributable to Van der Waals forces, covalent bond and hydrogen bond in the three-dimensional binding of hemicellulose, cellulose and lignin [38]. With increasing temperature and residence times, these interactions decrease or disappear as lignin degrades.

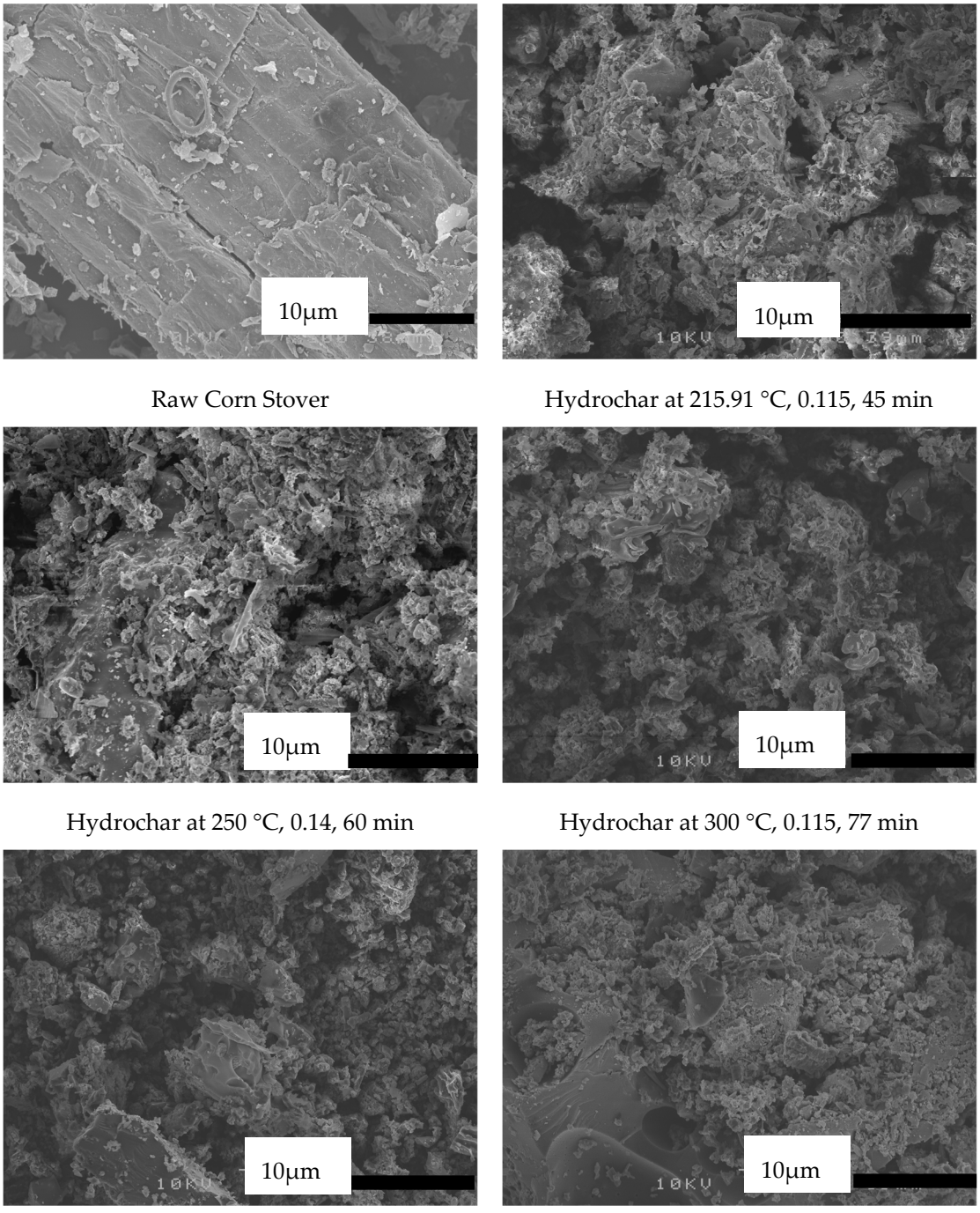

Raw Corn Stover

Hydrochar at 215.91 °C, 0.115, 45 min

Hydrochar at 250 °C, 0.14, 60 min

Hydrochar at 300 °C, 0.115, 77 min

Hydrochar at 350 °C, 0.14, 60 min

Hydrochar at 384.09 °C, 0.115, 45 min

Figure 3. Analysis of raw corn stover and solid fuels at 500× magnification.

3.1.2. Liquid Fraction

HPLC-RI analysis indicated that the major components of the liquid fraction were acetic acid, glycolic acid and ethanol. The concentrations of acetic acid, glycolic acid and ethanol ranged from 4.152 to 6.930 g/L, 1.410 to 5.11 g/L and 0.086 to 0.297 g/L, respectively (see Figure 4). The highest concentrations of acetic acid, glycolic acid and ethanol were achieved with a processing temperature of 250 or 350 °C, a constant biomass/water ratio of 0.14 and a residence time of 60 min. The acetic acid concentration increased with higher processing temperatures, while the glycolic acid concentration increased with longer residence times, likely as a result of the oxidation of glycoladehyde. Hemicellulose and cellulose are hydrolyzed into monosaccharides via the hydrothermal process [39]. These monosaccharides are unstable, and some of them are converted into other products such glycoladehyde, furfural and acetaldehyde, which in turn are converted to acetic acid (at high temperatures) and glycolic acid (at a longer residence time). The optimal processing conditions to produce acetic acid for an AD process is at a temperature of 350 °C, a biomass/water ratio of 0.14 and a residence time of 60 min. These conditions maximize the concentration of acetic acid in the liquid fraction; this result is desirable because acetic acid is the key feedstock for biomethane production via anaerobic digestion [23].

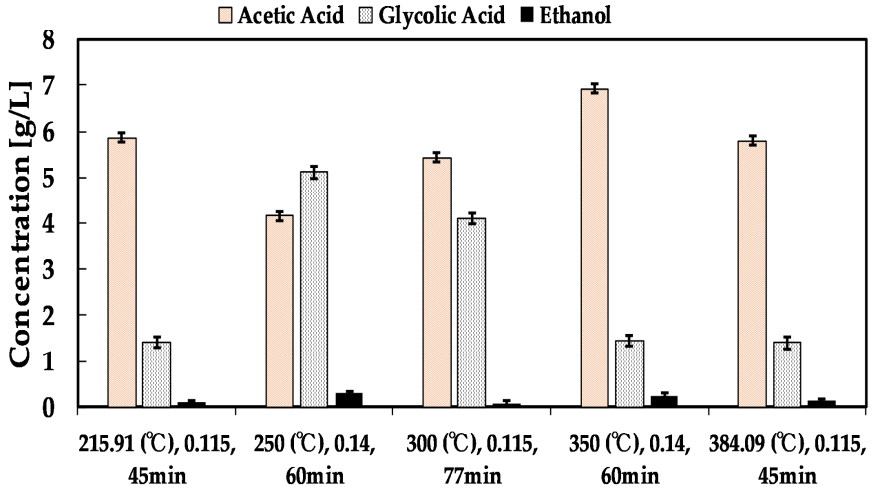

Figure 4. Concentration of acetic acid, glycolic acid and ethanol at different temperatures, residential times and biomass/water ratios. Each bar represents the mean ± standard deviation of results from three replications.

3.1.3. Gas Fraction

Gas yields from the HTC of corn stover as a function of the processing temperature, residence time and biomass/water ratio are presented in Figure 5. As the processing temperature was increased from subcritical water conditions to supercritical water conditions (215.91–384.09 °C), H_2 yield increased from 0.02 *v/v*% to 0.25 *v/v*%. The highest concentrations of CH_4 (0.135 *v/v*%) and CO_2 (3.5 *v/v*%) were also obtained with a processing temperature of 384.09 °C, residence time of 45 min and biomass/water ratio of 0.115, while the yield of CO yields was maximized at 250 °C, 60 min and 0.14 (0.085 *v/v*%). This is a result of CO reacting with water vapor in the water–gas shift reaction to liberate CO_2 and H_2 [40]. The water–gas shift reactions are favorable at high temperatures, mainly in supercritical water, and contribute to major yields of H_2 and CO_2 [41]. Supercritical water exists at a temperature and pressure above its critical point, which reduces its density and impedes ionic product formation. Free radical reactions become more facile near the critical point of water, therefore gasification (See Equation (5)) (steam reforming) and Equation (6) (water–gas shift reaction)) are favored to produce hydrogen and methane.

$$CH_4 + H_2O = CO + 3H_2 \; \Delta H_{298}{}^{\circ} = -205 \; kJ/mol \quad (5)$$

$$CO + H_2O = H_2 + CO_2 \Delta H_{298}^{\circ} = +42 \text{ kJ/mol} \quad (6)$$

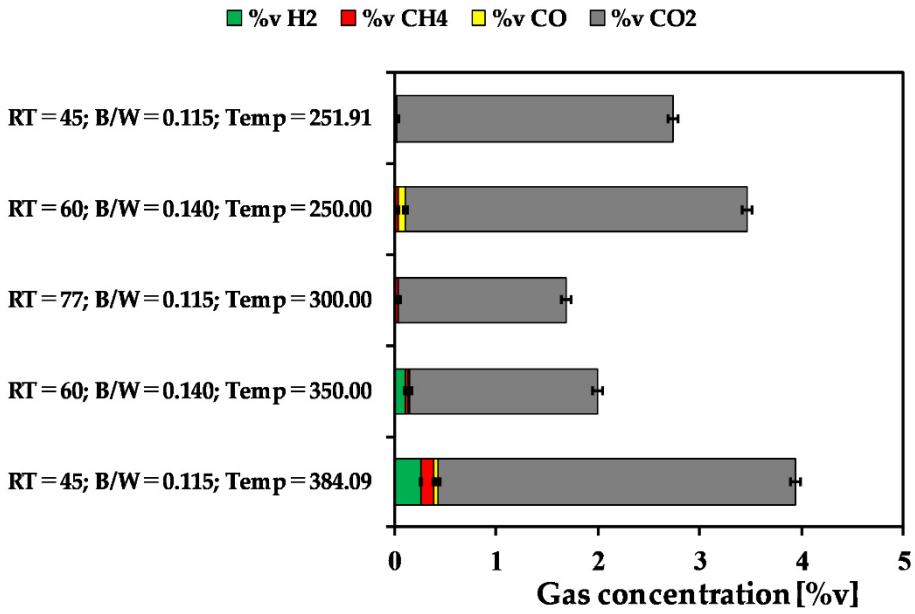

Figure 5. Concentration of gas at different temperature (Temp), residential time (RT) and biomass/water ratios (B/W). Each bar represents the mean ± standard deviation of result from three replication.

The formation of hydrogen is endothermic (Equation (6)) and the formation of methane is slightly exothermic (Equation (6)) [42]. Therefore, hydrogen formation dominates over methane formation at supercritical conditions, according to Le Chatlier's principle [43]. At 250 °C, 60 min and 0.14, the equilibrium position shifts in the exothermic direction, in which more water and carbon monoxide are formed, and hydrogen gas is present only in trace amounts. The CO concentration rises with increasing temperatures of up to 250 °C, and then drastically declines to >250 °C. The CO yield was higher than the yields of hydrogen and methane at processing temperatures between 225 and 280 °C. This result is like the findings of In-Gu et al. [44], and indicates that a significant amount of cellulose and other substrate in the corn stover was converted to CO over the temperature range 225–280 °C. Some carbon in the cellulose might have been gasified directly to form CO by pyrolysis. According to the report of In-Gu et al. [44], most of the cellulose in supercritical water is first disintegrated into biocrude (liquid phase) before being transformed into gaseous products. As the temperature is increased above 300 °C, the yields of carbon dioxide (CO_2) and hydrogen (H_2) increase and the production of CO drops off. These results confirm that the steam reforming and the water–gas shift reaction play a vital role in the production of hydrogen gas and methane.

3.2. Mechanism of Hydrothermal Carbonization

Our results confirm that the hydrothermal carbonization of corn stover induces hydrolysis, dehydration, aromatization, decarboxylation, polymerization and reforming reactions, as presented in Figure 6. The hydrochar is produced via two reaction pathways: (1) the cleavage of hemicellulose and cellulose into smaller compounds, such as pentose, hexose and polysaccharides, is caused by hydrolysis. The product obtained from hydrolysis undergoes a sequence of dehydration, fragmentation and isomerization reactions, forming the main intermediate Hydroxymethylfurfural and its derivative product. This intermediate further undergoes condensation and polymerization reactions associated with opposite intermolecular dehydration and aldol condensation [17,45]. The disintegration of this intermediate products also yields organic acid which comprises of formic, glycolic, acetic, propenoic and levulinic acids that reduced the reactions medium pH, and the condition of the solution (liquid phase) led to a gradual breakdown of the intermediate; in Figure 6, the gradual breakdown of hexoses

and pentose into furfurals and HMF can be seen [17,36,46]. The conversion process of polymers to solid fuel involves keto-enol tautomerism and intramolecular dehydration as a result of increased double bonds, which are favored via an aromatization reaction [3]. Hence, the aromatic cluster concentration in the liquid phase continues to increase as a result of an aromatization reaction, which reaches a critical point of saturation to form a burst nucleation [47]. The outward grows of the nuclei was formed by linkages and a diffusion of chemical compounds present in the liquid phase to the surface of nuclei; these linkages form a reactive functional group including oxygen and other elements such as quinines and ethers [47]. As the growth stopped, the external solid fuel particle contained a high concentration of reactive oxygen related to the core [3]. This solid fuel particle that comprises of a hydrophilic shell and hydrophobic core is in line with the findings of Sevilla et al. [47,48]. The furanic and arene proportion is formed at a high temperature and with a residence time. (2) The degradation of lignin to catechol (phenol) is also the result of hydrolysis; this intermediate undergoes cross-linking reactions and is polymerized into hydrochar; the insoluble lignin, which is not totally dissolved at low temperatures, undergoes a solid–solid reaction like pyrolysis, which produced a high condensed hydrochar with a polyaromatic structure [49]. The reaction in the HTC process favors solid–solid formations due to the small amount of soluble intermediate being used, which results in a low phenolics hydrochar [3]. At a temperature and pressure above the critical point of water, steam reforming and water–gas shift reactions occur to produce methane, hydrogen and carbon dioxide [44].

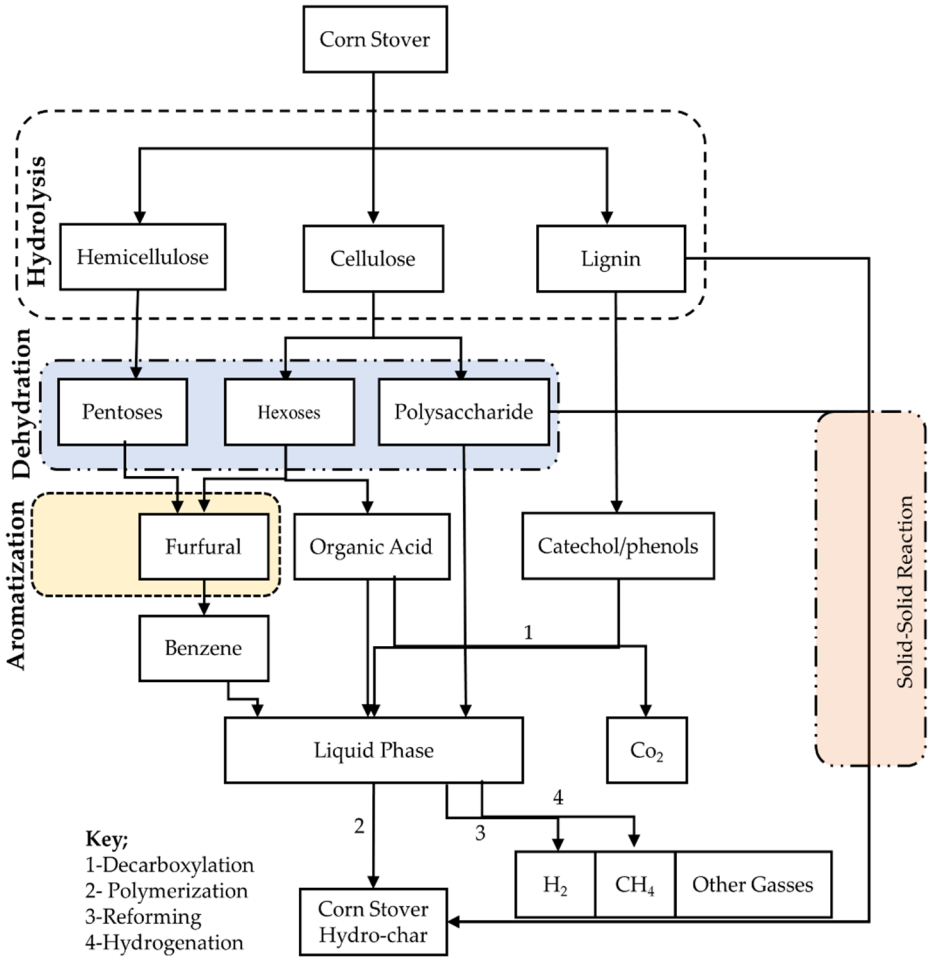

Figure 6. Pathways of the corn stover hydrochar formation mechanism [adapted from [22]].

3.3. Effect of Temperature, Residence Time, Biomass/Water Ratio on Corn Stover Hydrochar

The combined effects of the three process variables investigated on the properties of the hydrochar are visualized in Figure 7a–f. The response surface and contour plots of the interactions of processing temperature and residence time with respect to the HHV of the hydrochar at a fixed biomass/water ratio of 0.115 are presented in Figure 7a,b. The combined plots of temperature and residence time show the highest HHV of 26.03 MJ/kg at 300 °C and 77 min, while the minimum HHV of 16.37 MJ/kg is observed at 300 °C and 19 min 8 s. The results of the ANOVA test are presented in Table 4. Temperature and residence time are the most significant variables influencing the HHV [50]. This may be attributable to the fact that increased temperature and residence time improve the degree of intermediates dissolution and subsequent conversions through polymerization, leading to the formation of secondary char. This is the predominant mechanism of hydrochar formation (Figure 6). The HHV of the hydrochar decreases at a lower processing temperature and shorter residence time because low solid loading leads to a slow polymerization rate in the liquid phase, thereby limiting the formation of secondary hydrochar [51]. At supercritical conditions for water, the HHV (21.75 MJ/kg) of the hydrochar obtained was lower than the HHV of the hydrochar produced at subcritical conditions (26.03 MJ/kg). This may be a result of direct gasification of the corn stover constituents. The HHV of all the hydrochars was higher than raw corn stover; this result agrees with the results of [27,29].

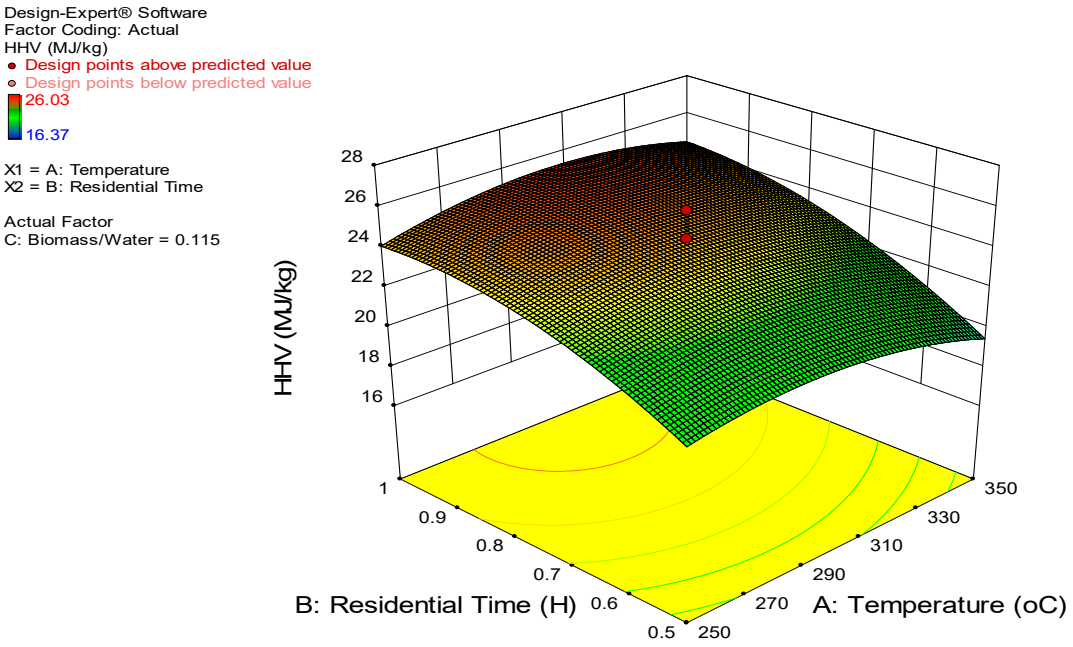

(**a**)

Figure 7. *Cont.*

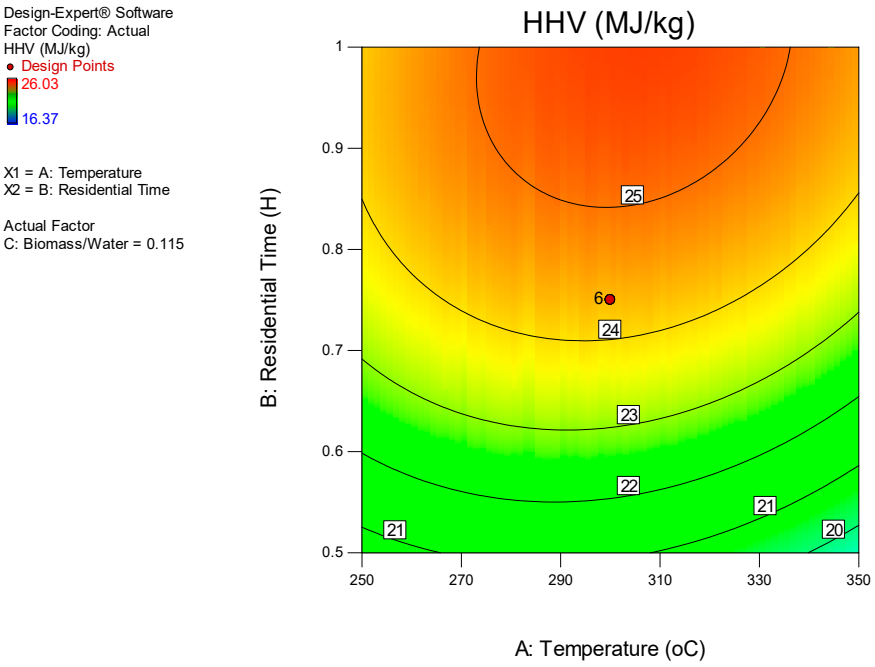

(**b**)

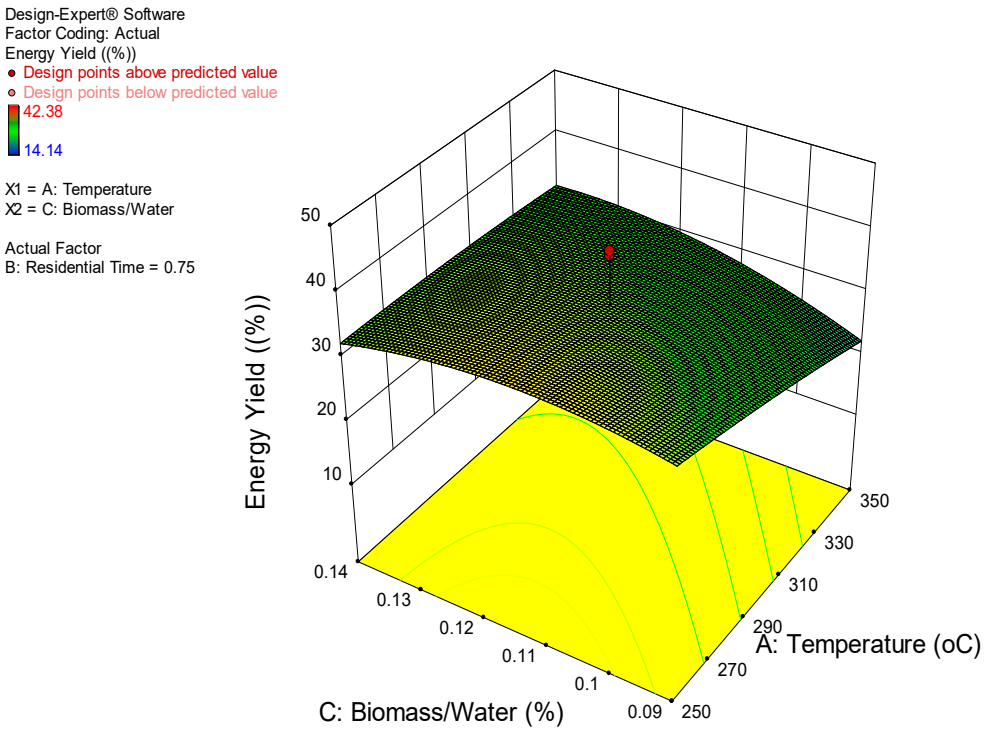

(**c**)

Figure 7. *Cont.*

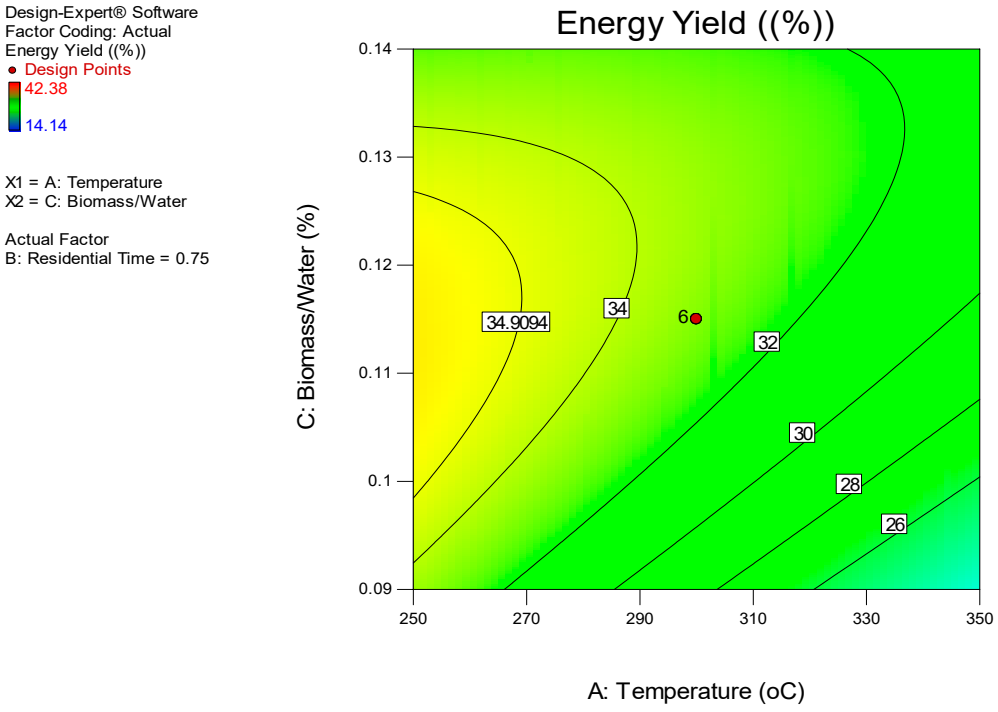

(**d**)

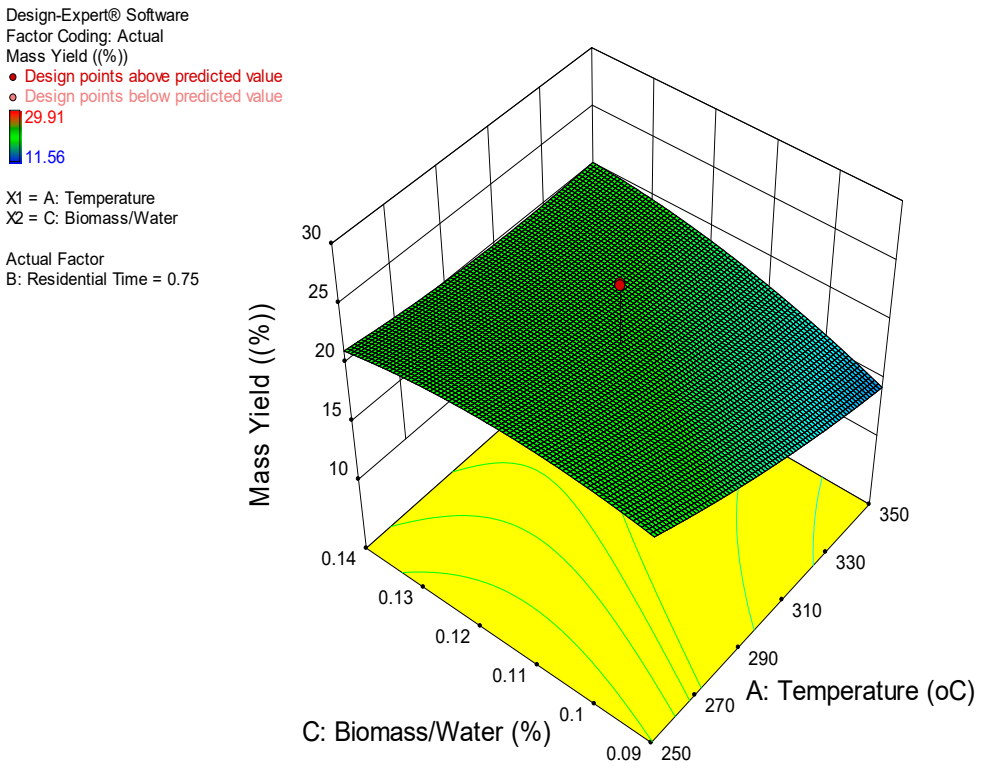

(**e**)

Figure 7. *Cont.*

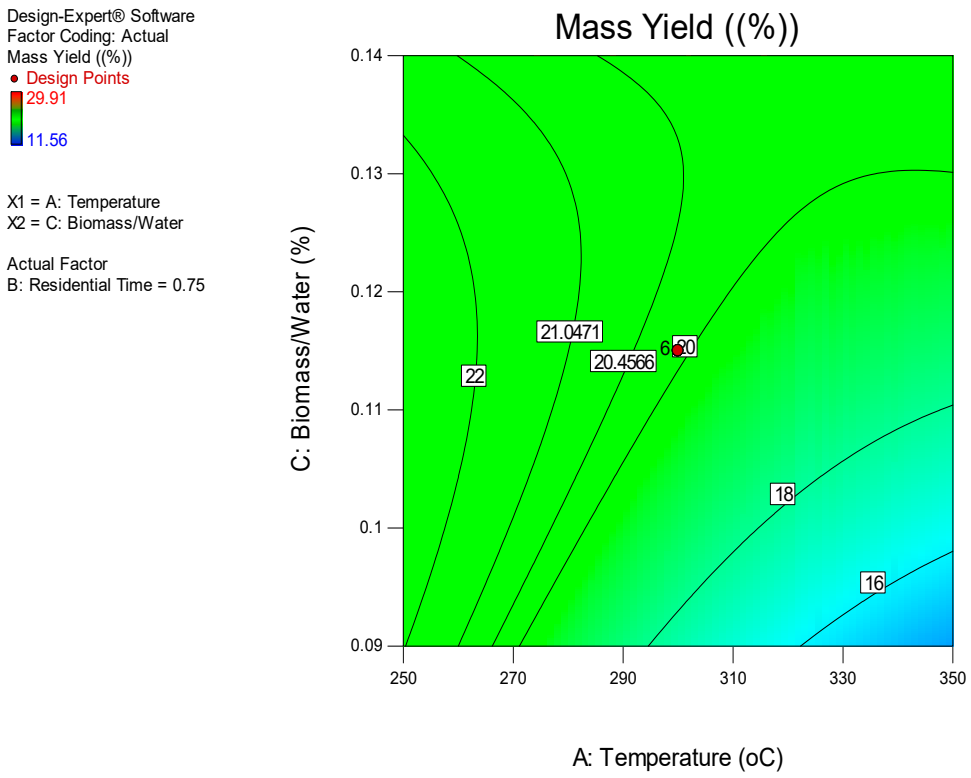

(**f**)

Figure 7. Surface and contour plots of high heating value (**a**,**b**), energy (**c**,**d**) and mass (**e**,**f**) yield.

Table 4. ANOVA for the high heating value [MJ/kg] response surface quadratic model.

Source	Sum of Squares	df	Mean Square	F-Value	P-Value	
Model	101.72	9	11.30	3.32	0.02	
X_1 -Temperature	5.63	1	5.63	1.65	0.03	
X_2 -Residential Time	54.19	1	54.19	15.91	0.00	
X_3 -Biomass/Water	0.65	1	0.65	0.19	0.02	
X_1X_2	0.49	1	0.49	0.14	0.01	
X_1X_3	1.08	1	1.08	0.32	0.05	significant
X_2X_3	0.10	1	0.10	0.03	0.02	
X_1^2	21.91	1	21.91	6.43	0.03	
X_2^2	18.05	1	18.05	5.30	0.01	
X_3^2	6.66	1	6.66	1.96	0.03	
Residual	34.05	10	3.41			
Lack of Fit	27.86	5	5.57	4.50	0.06	
Pure Error	6.19	5	1.24			
Cor Total	135.78	19				
Std Dev.	1.85	R^2	0.85			
Mean	19.15	AdJ-R^2	0.80			Not significant
C.V. %	9.63	Pred-R^2	0.70			
PRESS	231.49	Adeq-Precision	5.21			
-2Log Likelihood	67.40	BIC	97.36			
		AICc	111.85			

The effects of interactions between the processing temperature and biomass/water ratio (at a constant residence time of 45 min) on the energy yield of the hydrochar are illustrated in Figure 7c,d. The response surface and contour plot shows that as the temperature decreases from 384.09 to 215.9 °C, the energy yield increases from 29.88 wt.% to 42.38 wt.%, while at constant a temperature of 350 °C and residence time of 30 min, the energy yield increases from 14.14 wt.% to

26.40 wt.% with biomass/water ratios of 0.09 and 0.14, respectively. Both the processing temperature and biomass/water ratio display a strong influence on the hydrochar yield [50]. Increased temperatures enable a comprehensive decomposition of the corn stover and aid the deposition of carbon in the solid fuel. Lower biomass/water ratios also promote total disintegration of the corn stover, yielding a small amount of solid fuel [52].

Figure 7e,f depict the response surface and contour plots of the temperature and biomass/water ratio with respect to mass yield at a constant residence time of 45 min. Mass yield is a vital quantitative index that indicates how much the corn stover is transformed into solid fuel during HTC. The mass yield decreases as the temperature increases from 250 to 350 °C and biomass/water ratios change (0.09 to 0.14) because of the decomposition of the corn stover [50]. The increased temperature (>200 °C) weakens intramolecular hydrogen bonding in cellulose, increases the polarity of the CH_2OH group and promotes the cleavage of polysaccharides that form hydrochar via a solid–solid reaction (Figure 6). The highest mass yield obtained in this study was 29.91% with a processing temperature of 215.9 °C, a 45 min residence time and a biomass/water ratio of 0.115. Our results suggest that it is possible to manipulate processing conditions to adjust the mass loss of corn stover converted into liquid and gas fractions.

3.4. Hydrothermal Process Modelling and Optimization of Corn Stover Using RSM

The model for HHV detailed in Equation (7) was developed using RSM. The experimental data (Table 5) was used to fit the quadratic regression model of Equation (4), which describes the response of HHV to the independent experimental parameters of temperature, residence time and biomass/water ratios. The quadratic model was appraised by analysis of variances (ANOVA). The Fisher's test (F-value) and probability value (p-value) of the model are 3.32 and 0.02, respectively. Table 4 details the significances of the model at a 95% confident interval ($p < 0.05$). All quadratic, interaction and linear terms of the model equation were found to be significant. Performance assessments of the model were conducted using a statistical index ($R^2 = 0.85$ and adjusted $R^2 = 0.80$) that showed a good fit and correlation between the experimental and predicted data [22].

$$HHV\left[\frac{MJ}{kg}\right] = \begin{array}{c} -52.849 + 0.302 * X_1 + 26.77 * X_2 + 316.06 * X_3 + 0.0198 * X_1X_2 \\ - 0.2943 * X_1X_2 + 18.291 * X_2X_3 - 4.93x10^{-4} * X_1^2 - 17.905 * X_2^2 \\ - 1087.89 * X_3^2 \end{array} \quad (7)$$

The optimization and validation results for the HHV of corn stover hydrochar are presented in Table 5. The predicted responses were formulated by employing a point prediction node beneath the optimization node in the CCD. Process variables included the temperature, residence time and biomass/water ratio in the ranges of 250–350 °C, 0.5–1 h and 0.09–0.114, respectively. HHV was maximized within the experimental range of 16.37–26.03 MJ/kg and the optimal conditions were suggested by the software at a desirability value of 0.937. Experimental validation of the optimal conditions was conducted in triplicate; a maximum HHV of 25.73 MJ/kg was obtained, which was 7.75% less than the predicted value. The experimental value was within the variance ranges of ±10 %. The difference between the experimental and predicted result may stem from the adjusted R^2 of 0.80 in the quadratic model.

Table 5. Response and variables condition of HTC process optimization experiment, and average values of HHV, energy yield and mass yield.

Run	Temperature	Residence Time (h)	Biomass/Water Ratio	Final Pressure (Mpa)	HHV (MJ/kg)	Energy Yield (%)	Mass Yield (%)
1	300	0.75	0.157	14.95	20.73	28.48	20.23
2	300	0.75	0.115	15.95	25.85	31.45	17.91
3	300	0.75	0.115	14.99	23.70	31.26	19.42
4	350	1	0.09	22.45	21.95	19.21	12.89
5	300	0.75	0.115	15.75	24.49	41.46	24.93
6	300	0.75	0.073	12.25	23.23	31.03	19.66
7	384.09	0.75	0.115	26	21.75	29.88	20.23
8	300	0.33	0.115	15.95	16.37	28.36	25.51
9	250	0.5	0.09	10.35	19.85	31.19	23.13
10	250	1	0.14	10.50	23.08	30.16	19.24
11	300	0.75	0.115	15.75	24.05	27.94	17.10
12	215.91	0.75	0.115	8.85	20.86	42.38	29.91
13	300	0.75	0.115	15.25	24.19	24.67	15.01
14	300	0.75	0.115	16	23.91	40.76	25.10
15	250	1	0.09	10.40	23.20	22.88	14.52
16	300	1.170	0.115	16	26.03	40.90	23.13
17	350	1	0.14	23.2	23.93	32.97	20.29
18	250	0.5	0.14	20	19.82	26.40	19.61
19	250	0.5	0.14	10.50	21.44	29.68	20.38
20	350	0.5	0.09	23	18.01	14.14	11.56
Raw Samples					14.72		
HHV (Optimum)	305	1	0.14	16.34	25.42	-	-
HHV (Validated)	305	1	0.14	16.34	24.45	-	-
Standard deviation (%)					0.016	0.017	0.018

4. Conclusions

This study demonstrates that corn stover can be converted to solid fuel through HTC. The corn stover hydrochar has a high degree of coalification because of its high processing temperature and long residence time. CCD-RSM was used to optimize processing conditions. The effect of the temperature, residence time and biomass/water ratio on the properties of the hydrochar were also examined. The optimal processing parameters predicted using the model were a temperature of 305 °C, residence time of 60 min, biomass/water ratio of 0.114 and a pressure of 16.25 MPa. These conditions were validated experimentally and found to be within 0.0097% of the predicted result. The ANOVA test revealed that temperature and residence time were the most significant variables that affect hydrochar yield.

SEM, TGA and DTG were used to reveal significant changes in the morphology, weight loss and thermal stability of corn stover hydrochar. Our results indicate that hydrochar produced at 300 °C contains the highest amount of fixed carbon.

HPLC analysis of the liquid fraction revealed that it contains high concentrations of acetic acid (up to 6.970 g/L). The hydrothermal liquid will be used in an anaerobic digestion in future work entailing process modeling, control, simulation and optimization of a biomethane production management system.

The yields of H_2, CO_2 and CH_4 in the gas fraction are higher at supercritical conditions than at subcritical conditions. The HHV of the hydrochar is higher at subcritical conditions (26.03 MJ/kg) than at supercritical conditions (21.75 MJ/kg). The highest mass and energy yields (29.91% and 42.38%, respectively) were obtained with the following processing parameters: a residence time of 45 min, biomass/water ratio of 0.115, processing temperature of 215.91 °C and pressure of 8.85 MPa.

Author Contributions: Conceptualization, I.S.M. and N.S.; methodology, I.S.M., R.N. and K.K.; software, I.S.M.; writing-original draft preparation, I.S.M. and N.S.; writing-review and editing N.S., and I.S.M.; All authors have read and agreed to the published version of the manuscript.

Funding: This research received no external funding.

Acknowledgments: The HPLC-RI and TGA/DTG analysis was performed by the instrumental analysis service of the Global facility Center of Hokkaido University. We thank Edanz Group (https://en-author-services.edanzgroup.com/) for editing a draft of this manuscript.

Conflicts of Interest: The authors declare no conflict of interest.

Future Work: The liquid fraction obtained from HTC process will be utilized as a substrate in anaerobic digestion (AD) system to generate biogas driven data. This data will be used to develop a model that will describe the dynamics of the AD system online.

References

1. Chew, J.J.; Doshi, V. Recent advances in biomass pretreatment–Torrefaction fundamentals and technology. *Renew. Sustain. Energy Rev.* **2011**, *15*, 4212–4222. [CrossRef]
2. Hastings, A.; Clifton-Brown, J.; Wattenbach, M.; Mitchell, C.P.; Stampfl, P.; Smith, P. Future energy potential of Miscanthusin Europe. *GCB Bioenergy* **2009**, *1*, 180–196. [CrossRef]
3. Akhtar, J.; Amin, N.A.S. A review on process conditions for optimum bio-oil yield in hydrothermal liquefaction of biomass. *Renew. Sustain. Energy Rev.* **2011**, *15*, 1615–1624. [CrossRef]
4. Mohammed, I.S.; Aliyu, M.; Abdullahi, N.A.; Alhaji, I.A. Production of bioenergy from rice-melon co-digested with cow dung as inoculant. *Agri. Eng. Int. CIGR J.* **2020**, *22*, 108–117.
5. Anca-Couce, A. Reaction mechanisms and multi-scale modelling of lignocellulosic biomass pyrolysis. *Prog. Energy Combust. Sci.* **2016**, *53*, 41–79. [CrossRef]
6. Himmel, M.E.; Ding, S.Y.; Johnson, D.K.; Adney, W.S.; Nimlos, M.R.; Brady, J.W. Biomass recalcitrance: Engineering plants and enzymes for biofuels production. *Science* **2007**, *315*, 804–807. [CrossRef] [PubMed]
7. Paul, S.; Dutta, A.; Defersha, F. Biocarbon, biomethane and biofertilizer from corn residue: A hybrid thermo-chemical and biochemical approach. *Energy* **2018**, *165*, 370–384. [CrossRef]
8. Zhao, P.; Shen, Y.; Ge, S.; Yoshikawa, K. Energy recycling from sewage sludge by producing solid biofuel with hydrothermal carbonization. *Energy Convers. Manag.* **2014**, *78*, 815–821. [CrossRef]
9. Pala, M.; Kantarli, I.C.; Buyukisik, H.B.; Yanik, J. Hydrothermal carbonization and torrefaction of grape pomace: A comparative evaluation. *Bioresour. Technol.* **2014**, *161*, 255–262. [CrossRef]
10. Reza, M.T.; Rottler, E.; Herklotz, L.; Wirth, B. Hydrothermal carbonization (HTC) of wheat straw: Influence of feedwater pH prepared by acetic acid and potassium hydroxide. *Bioresour. Technol.* **2015**, *182*, 336–344. [CrossRef]
11. Cai, J.; Li, B.; Chen, C.; Wang, J.; Zhao, M.; Zhang, K. Hydrothermal carbonization of tobacco stalk for fuel application. *Bioresour. Technol.* **2016**, *220*, 305–311. [CrossRef] [PubMed]
12. Volpe, M.; Fiori, L. From olive waste to solid biofuel through hydrothermal carbonization: The role of temperature and solid load on secondary char formation and hydrochar energy properties. *J. Anal. Appl. Pyrolysis* **2017**, *124*, 63–72. [CrossRef]
13. Erdogan, E.; Atila, B.; Mumme, J.; Reza, M.T.; Toptas, A.; Elibol, M.; Yanik, J. Characterization of products from hydrothermal carbonization of orange pomace including anaerobic digestibility of process liquor. *Bioresour. Technol.* **2015**, *196*, 35–42. [CrossRef] [PubMed]
14. Wikberg, H.; Ohra-aho, T.; Honkanen, M.; Kanerva, H.; Harlin, A.; Vippola, M.; Laine, C. Hydrothermal carbonization of pulp mill streams. *Bioresour. Technol.* **2016**, *212*, 236–244. [CrossRef]
15. Deng, J.; Li, M.; Wang, Y. Biomass-derived carbon: Synthesis and applications in energy storage and conversion. *Green Chem.* **2016**, *18*, 4824–4854. [CrossRef]
16. Gao, Y.; Xian-Hua, W.; Hai-Ping, Y.; Han-Ping, C. Characterization of products from hydrothermal treatments of cellulose. *Energy* **2012**, *42*, 457–465. [CrossRef]
17. Funke, A.; Ziegler, F. Hydrothermal carbonization of biomass: A summary and discussion of chemical mechanisms for process engineering. *Biofuels Bioprod. Biorefin.* **2010**, *4*, 160–177. [CrossRef]
18. Hu, B.; Wang, K.; Wu, L.; Yu, S.H.; Antonietti, M.; Titirici, M.M. Engineering carbon materials from the hydrothermal carbonization process of biomass. *Adv. Mater.* **2010**, *22*, 813–828. [CrossRef]
19. Kang, S.; Ye, J.; Zhang, Y.; Chang, J. Preparation of biomass hydrochar derived sulfonated catalysts and their catalytic effects for 5-hydroxymethylfurfural production. *RSC Adv.* **2013**, *3*, 7360–7366. [CrossRef]
20. Steinbeiss, S.; Gleixner, G.; Antonietti, M. Effect of biochar amendment on soil carbon balance and soil microbial activity. *Soil Biol. Biochem.* **2009**, *41*, 1301–1310. [CrossRef]
21. Kruse, A.; Funke, A.; Titirici, M.M. Hydrothermal conversion of biomass to fuels and energetic materials. *Curr. Opin. Chem. Biol.* **2013**, *17*, 515–521. [CrossRef] [PubMed]

22. Mohammed, I.S.; Aliyu, M.; Dauda, S.M.; Balami, A.A.; Yunusa, B.K. Synthesis and optimization process of ethylene glycol-based biolubricant from palm kernel oil (PKO). *JREE Spring* **2018**, *5*, 2–8.
23. Zhu, Z.; Zhidan, L.; Yuanhui, Z.; Baoming, L.; Haifeng, L.; Na, D.; Buchun, S.; Ruixia, S.; Jianwen, L. Recovery of reducing sugars and volatile fatty acids from cornstalk at different hydrothermal treatment severity. *Bioresour. Technol.* **2016**, *199*, 220–227. [CrossRef] [PubMed]
24. Machado, N.T.; de Castro, D.A.R.; Santos, M.C.; Araújo, M.E.; Lüder, U.; Herklotz, L.; Werner, M.; Mumme, J.; Hoffmann, T. Process analysis of hydrothermal carbonization of corn Stover with Subcritical water. *J. Supercrit. Fluids* **2018**, *136*, 110–122. [CrossRef]
25. Mosier, N.; Richard, H.; Nancy, H.; Miroslav, S.; Michael, R.L. Optimization of pH controlled liquid hot water pretreatment of corn stover. *Bioresour. Technol.* **2005**, *96*, 1986–1993. [CrossRef]
26. Fuertes, A.B.; Camps, A.M.; Sevilla, M.; Maciá-Agulló, J.A.; Fiol, S.; López, R.; Smernik, R.J.; Aitkenhead, W.P.; Arce, F.; Macias, F. Chemical and structural properties of carbonaceous products obtained by pyrolysis and hydrothermal carbonization of corn stover. *Aust. J. Soil Res.* **2010**, *48*, 618–626. [CrossRef]
27. Xiao, L.; Zheng-Jun, S.; Feng, X.; Run-Cang, S. Hydrothermal carbonization of lignocellulosic biomass. *Bioresour. Technol.* **2012**, *18*, 619–623. [CrossRef]
28. Volpe, M.; Jillian, L.G.; Luca, F. Hydrothermal carbonization of Opuntia ficus-indica cladodes: Role of process parameters on hydrochar properties. *Bioresour. Technol.* **2018**, *247*, 310–318. [CrossRef]
29. Kang, K.; Sonil, N.; Guotao, S.; Ling, Q.; Yongqing, G.; Tianle, Z.; Mingqiang, Z.; Runcang, S. Microwave-assisted hydrothermal carbonizatijon of corn stalk for solid biofuel production: Optimization of process parameters and characterization of hydrochar. *Energy* **2019**, *186*, 115–125. [CrossRef]
30. Ushiyama, T.; Shimizu, N. Microencapsulation using spray-drying: The use of fine starch solution for the wall material. *Food Sci. Technol. Res.* **2018**, *24*, 653–659. [CrossRef]
31. Shimizu, N.; Abea, A.; Ushiyama, T.; Toksoy Öner, E. Effect of temperature on the hydrolysis of levan treated with compressed hot water fluids. *Food Sci. Nutr.* **2020**, *8*, 1–11. [CrossRef]
32. Athika, C.; Tau, L.Y.; Shigeru, M.; Yukihiko, M. Behavior of 5-HMF in Subcritical and Supercritical Water. *Ind. Eng. Chem. Res.* **2008**, *47*, 2956–2962.
33. Chandra, S.T.; Jason, S.M. Hydrothermal liquefaction of separated dairy manure for production of bio-oils with simultaneous waste treatment. *Bioresour. Technol.* **2012**, *107*, 456–463. [CrossRef]
34. Kambo, H.S.; Dutta, A. Comparative evaluation of torrefaction and hydrothermal carbonization of lignocellulosic biomass for the production of solid biofuel. *Energy Convers. Manag.* **2015**, *105*, 746–755. [CrossRef]
35. Kamonwat, N.; Bunyarit, P.; Vorapot, K.; Nawin, V.; Wasawat, K.; Prasert, P. Characteristics of hydrochar and liquid fraction from hydrothermal carbonization of cassava rhizome. *J. Energy Inst.* **2018**, *91*, 184–193.
36. Hoekman, S.K.; Broch, A.; Robbins, C. Hydrothermal carbonization (HTC) of lignocellulosic biomass. *Energy Fuels* **2015**, *25*, 1802–1810. [CrossRef]
37. Elaigwu, S.E.; Greenway, G.M. Microwave-assisted and conventional hydrothermal carbonization of lignocellulosic waste material: Comparison of the chemical and structural properties of the hydrochars. *J. Anal. Appl. Pyrolysis* **2016**, *118*, 1–8. [CrossRef]
38. Cantero, D.A.; Martinez, C.; Bermejo, M.D.; Cocero, M.J. Simultaneous and selective recovery of cellulose and hemicellulose fractions from wheat bran by supercritical water hydrolysis. *Green Chem.* **2015**, *17*, 610–618. [CrossRef]
39. Abdullah, R.; Ueda, K.; Saka, S. Hydrothermal decomposition of various crystalline celluloses as treated by semi-flow hot-compressed water. *J. Wood Sci.* **2014**, *60*, 278–286. [CrossRef]
40. Kruse, A. Supercritical water gasification. *Biofuels Bioprod. Bioref.* **2008**, *2*, 415–437. [CrossRef]
41. Reddy, S.N.; Nanda, S.; Dalai, A.K.; Kozinski, J.A. Supercritical water gasification of biomass for hydrogen production. *Int. J. Hydrog. Energy* **2014**, *39*, 6912–6926. [CrossRef]
42. De Vlieger, D.J.M.; Chakinala, A.G.; Lefferts, L.; Kersten, S.R.A.; Seshan, K.; Brilman, D.W.F. Hydrogen from ethylene glycol by supercritical water reforming using noble and base metal catalysts. *Appl. Catal. B Environ.* **2012**, *112*, 536–544. [CrossRef]
43. Liu, Z.; Quek, A.; Kent, S.; Hoekman, R.B. Production of solid biochar fuel from waste biomass by hydrothermal carbonization. *Fuel* **2013**, *103*, 943–949. [CrossRef]
44. In-Gu, L.; Mi-Sun, K.; Son-Ki, I. Gasification of Glucose in Supercritical Water. *Ind. Eng. Chem. Res.* **2002**, *41*, 1182–1188.

45. Kumar, S. Sub-and supercritical water technology for biofuels. In *Advanced Biofuels and Bioproducts*; Springer: New York, NY, USA, 2013; pp. 147–183.
46. Falco, C.N.B.; Titirici, M.M. Morphological and structural differences between glucose, cellulose and lignocellulosic biomass derived hydrothermal carbons. *Green Chem.* **2011**, *13*, 3273–3281. [CrossRef]
47. Sevilla, M.; Fuertes, A.B. The production of carbon materials by hydrothermal carbonization of cellulose. *Carbon* **2009**, *47*, 2281–2289. [CrossRef]
48. Sevilla, M.; Fuertes, A.B. Chemical and structural properties of carbonaceous products obtained by hydrothermal carbonization of saccharides. *Chem. A Eur. J.* **2009**, *15*, 4195–4203. [CrossRef] [PubMed]
49. Fang, Z.; Sato, T.; Smith, R.L.; Inomata, H.; Arai, K.; Kozinski, J.A. Reaction chemistry and phase behavior of lignin in high-temperature and supercritical water. *Bioresour. Technol.* **2008**, *99*, 3424–3430. [CrossRef]
50. Tengfei, W.; Yunbo, Z.; Yun, Z.; Caiting Li Guangming, Z. A review of the hydrothermal carbonization of biomass waste for hydrochar formation: Process conditions, fundamentals, and physicochemical properties. *Renew. Sustain. Energy Rev.* **2018**, *90*, 223–247. [CrossRef]
51. Fan, J.; De bruyn, M.; Budarin, V.L.; Gronnow, M.J.; Shuttleworth, P.S.; Breeden, S. Direct microwave-assisted hydrothermal depolymerization of cellulose. *J. Am. Chem. Soc.* **2013**, *135*, 11728–11731. [CrossRef]
52. He, C.; Giannis, A.; Wang, J.Y. Conversion of sewage sludge to clean solid fuel using hydrothermal carbonization: Hydrochar fuel characteristics and combustion behavior. *Appl. Energy* **2013**, *111*, 257–266. [CrossRef]